

PHYSICS OF FLUIDS

<https://aip.scitation.org/journal/phf>

Accepted May 20th 2022

THERMAL EFFECTS ON SARS-COV-2 TRANSMISSION IN PERISTALTIC BLOOD FLOW: MATHEMATICAL MODELLING

***¹Dharmendra Tripathi, ¹D. S. Bhandari and ²O. Anwar Bég**

¹*Department of Mathematics, National Institute of Technology, Uttarakhand -246174, India*

²*Multi-Physical Engineering Sciences Group, Dept. Mechanical and Aeronautical Engineering, SEE, Salford University, Manchester, M54WT, UK.*

**Corresponding author: dtripathi@nituk.ac.in*

ABSTRACT

SARS-CoV-2 is a novel viral species that has been identified as a highly infectious disease. Scientists have endeavored to collect essential information to characterize better the behaviour of this virus including droplet transmission and airborne effects. However, it is not clear thus far whether temperature can substantially alter the pandemic trajectory inside the physiological system. The present study aims to investigate how temperature may affect virus transmission in peristaltic blood vessels, and how virus density and diameter, and blood viscosity (i.e. viscosity of carrying fluids) will affect the transmission of the virus in the circulatory system. The modelling deployed assumes that coronavirus with a diameter of $120\mu m$ and a density of $1g/cm^3$ move in the direction of blood flow. The quantity of SARS-CoV-2 virions (entire virus particles) inside a microdroplet is calculated by considering the Kepler conjecture method, and the transmission percentage of viral load is also computed. It is observed that the microdroplet carries less amount of coronavirus particles, so an airborne particle ($D_p < 2\mu m$) infection is less harmful. Further, computational simulations using the proposed model reveal some interesting insights into how rapidly the SARS-CoV-2 virus propagates in the circulatory system and estimate the infection in blood vessels. From these results, it is found that the small virion ($d_p < 100nm$) rapidly settles inside the bloodstream and infects tissues; however, the duration of infection is short due to the low viscosity of the blood. Further, the closed packed structure of the virions is loosened in the blood vessel due to blood temperature.

Keywords: *Boussineq-Basset equation; coronavirus; packing density; heat transfer; peristaltic blood flow.*

Nomenclature

f_i	hydrodynamic force (N)
U_i	velocity of blood flow (m/s)
V_i	velocity vector of the virion (m/s)
L	length of the blood vessel (m)
m	mass of the fluid (kg)
m_p	mass of the virion (kg)
p	blood pressure (Pa)
g	gravitational acceleration (m/s^2)
c	wave velocity (m/s)
t	time scale (s)
T_0, T_1	temperature at the centre and wall respectively (K)
u, v	velocity components in the x, y directions respectively (m/s)
r	radius of the virion (nm)
d_p	virion diameter (nm)
D_p	droplet diameter (nm)
N_p	number of virions (-)
R_w	width of the blood vessel (m)
τ_p	particle relaxation time (s)
τ_c	fluid (blood) characteristic time (s)
Φ	specific heat source (W/m^2)
θ	temperature (K)
ε	wave number (-)
Φ	stream function (-)
β	heat source parameter (-)

Dimensionless Parameters

Pr	Prandtl number (-)
Gr	Grashof number (-)
Re	Reynolds number (-)

T_p	transmission of virions (-)
V_T	percentage of virion transmission (-)
S_N	Stokes number (-)
S	density ratio (-)
β_1	drag force parameter (-)
β_2	virtual mass parameter (-)
β_3	Basset parameter (-)
β_4	gravity parameter (-)

1 Introduction

In 2019, SARS-CoV-2 spread rapidly across the world and emerged as a global pandemic. It caused infection of the respiratory system in humans that can vary from mild to lethal. With time, this virus has mutated into different strains and has taken many lives. Significant public safety measures were introduced to maintain control of the pandemic. In parallel, scientists attempted to assess and control key aspects of the virus including droplet transmission. The first species of this virus appeared in 1966 [1], which was identified as two abnormal human respiratory viruses such as CoV-229E and CoV-B814. These viruses were found in a spherical shape of size 80 – 120 nm in diameter through fluorescence and electron microscopy as shown in **Figure 1** (See Ref. [1]). Further studies showed that the droplet of virus particles do not settle with a size below $5\mu m$ which allows the virus particles to remain active in the air for a long time [2]. Some studies reported that the small size droplet of the virion evaporates due to humidity and temperature effects [3, 4]. In the context of SARS-CoV-2, researchers have discussed the outbreak of virus infection due to its seasonal nature [3, 5, 6]. However, a proper characterization of the impact of these parameters has remained elusive.

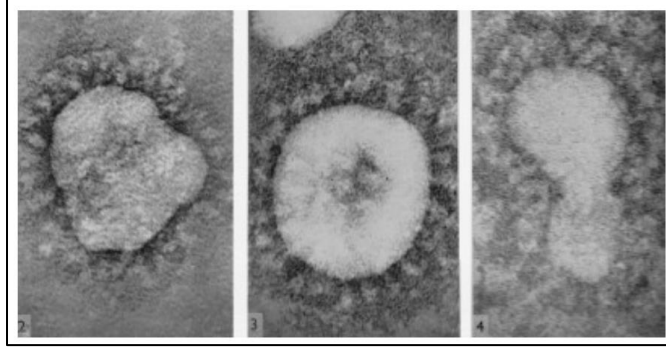


Figure 1: Electron microscope images of coronaviruses 229E and B814 (See Ref. [1]).

It is important to understand all the aspects that can control the spread of SARS-CoV-2. The behavior of virus particles inside the human body involves complex flow phenomena. The physical interpretation of virus transport inside blood vessels is essential for determining the transmission of coronavirus in the circulatory system. Furthermore, given the importance of flow phenomena in the transmission process, the methods, equipment, and practices employed to mitigate respiratory infections also involve fluid dynamics. In this regard, Maxey and Riley [7] have developed an expression for the motion of a particle inside a viscous fluid, using the Boussinesq-Basset equation as:

$$\frac{m_p d\bar{V}_i}{d\bar{t}} = (m_p - m)\bar{g} + m \frac{D\bar{U}_i}{D\bar{t}} + f_i \quad (1)$$

Here $\bar{V}_i = (u_p, v_p)$ is the velocity vector of the virus particle, \bar{U}_i is the fluid velocity, f_i is the hydrodynamic force exerted by the flow field. m_p is the particle mass, m is the mass of the fluid, \bar{g} is the gravity vector. The second term ($m \frac{D\bar{U}_i}{D\bar{t}}$) is a purely inertial contribution, which is the so-called added mass. It represents the additional mass that particles appear to possess due to the resistance to the acceleration of the surrounding fluid. The last term, f_i is also known as *disturbance force* occurring in the fluid due to the particles, and is expressed as follows:

$$f_i = -\frac{1}{2}m_i\{\bar{V}_i - \bar{U}_i\} - 6\pi r\mu\{\bar{V}_i - \bar{U}_i\} - 6\pi r^2\mu\left(\int_0^{\bar{t}} \frac{\left(\frac{d}{d\bar{t}}(\bar{V}_i - \bar{U}_i)\right)}{\sqrt{(\pi\nu(\bar{t}-\tau))}} d\tau + \frac{(v_{i0} - \bar{U}_i)}{\sqrt{\bar{t}}}\right) \quad (2)$$

The equation of particle motion associated with the hydrodynamic force in viscous flow is the sum of the steady-state drag force, the added mass force, and the Basset force. Generally, the Basset-Boussinesq expression describes the motion of a particle under the transient hydrodynamic force

exerted by Stokes drag and Basset force. Another concept of particle-fluid motion in two phases i.e. fluid phase and particulate phase was introduced in the literature to examine the particle motion based on the continuity and momentum equation without using the Boussinesq-Basset equation. The two phase particle-fluid motion based on mathematical models [8-10] have been reported and discussed the dusty fluid flow with various rheological properties. A virus laden particle motion over urinal flushing is simulated and mesh sensitivity analysis was performed [11]. They have reported that anti-diffusion improvements of facilities in public washrooms are required. Using the nano-particle transport equations, Islam et al. [12] analyzed how far SARS-CoV-2 particles can travel in the respiratory system and have reported that “the majority of SARS-CoV-2 aerosols are trapped at RL and RU lobes, and the minority is trapped at RM and LU lobes for 7.5 and 30 l/min airflow rates.” Islam et al. [13] further demonstrated how coronavirus-2 aerosol propagates through age-specific upper airways. Finlay [14] presented the mechanics of the aerosol - in his book chapter-3 describes the motion of a single aerosol in a fluid medium. Holländer and Zaripov [15] investigated interactions of monodisperse $73\mu m$ geometric diameter droplets with initial velocities between 1.5 and $3m/s$ with the inclusion of the Basset force based on the Maxey-Riley derivation [7]. Smith et al. [16] illustrated that highly infected people having a large viral load in their saliva and superspreaders producing lots of aerosols are likely to be far more dangerous transmitters of infection. Various studies [7-16] have reported on the movement of particles, aerosols, viruses, and droplets using diverse approaches, particularly with different formulations of the particle motion equation. However, no study has examined theoretically so far the virus movement in circulatory systems under the thermal effects and/or considered the simultaneous effects of blood viscosity, virus density and diameter with peristaltic pumping.

To develop a novel mathematical model for the propagation of coronavirus through blood flow, we investigate theoretically the transient motion of particles in viscous flow with heat transfer through a peristaltic channel, as a model of coronavirus transmission in peristaltic blood flow. Peristalsis is achieved via the rhythmic contraction and expansion of the walls of a distensible conduit which generates efficient propulsion in blood flow and many other biological and bio-inspired applications [17-22]. In the present study, the kinematics of the channel wall induce the flow under peristaltic waves. The modelling deployed assumes that coronavirus particles with a diameter of $120\mu m$ and a density of $1g/cm^3$ move in the direction of blood flow. The quantity

of SARS-CoV-2 virions (entire virus particles) inside a microdroplet is calculated by considering the Kepler conjection method and the transmission percentage of viral load is also computed. Expressions are derived for the axial and transverse velocity of a coronavirus particle. Computations are performed to visualize the streamline profiles, variation in the particle relaxation time with particle diameter, and distribution of the number of virions (N_p) with SARS-CoV-2 diameter $d_p(nm)$ for different particle diameters and also the evolution of transmission virions (T_p) with SARS-CoV-2 diameter $d_p(nm)$ for different virion transmission percentages (V_T). The study provides novel observations which will aid in understanding how coronavirus transmits through blood flow in the circulatory system under the effects of thermal variation and rheological properties of different human blood characteristics. Here we attempt to use well-established mathematical tools from fluid dynamics to understand why some individuals remain asymptomatic whereas some die from COVID-19 infection. Furthermore, our analyses also partly explain the differential rate of clinical symptoms from the time since infection within severe cases [23].

2 Mathematical Model

2.1 Governing equations

The modelling approach deployed herein adopts lubrication theory i.e., blood flow occurs in a characteristic length of blood vessel much greater than the typical radius. **Figure 2** depicts the virus transmission in blood flow through a vertical deformable vessel. Since a key objective of this study is to examine the influence of thermal effects on the transport of virus through peristaltic blood flow, heat transfer analysis is included in the present model. The governing equations for the present biophysical model may be defined in vectorial form as follows:

$$\nabla \cdot \bar{U}_i = 0 \quad (3)$$

$$\rho \left(\frac{\partial \bar{U}_i}{\partial \bar{t}} + \bar{U}_i \cdot \nabla \bar{U}_i \right) = -\nabla \bar{p} + \mu (\nabla^2 \bar{U}_i) + \rho g \alpha (T - T_0) \quad (4)$$

$$\rho c_p \left(\frac{\partial \bar{T}}{\partial \bar{t}} + \nabla \cdot (\bar{V}_f \bar{T}) \right) = \nabla \cdot (k \nabla \bar{T}) + \Phi \quad (5)$$

where \bar{t} , and \bar{p} symbolize time, and pressure, respectively. Blood is considered to be Newtonian with a density (ρ) of $1050 kg/m^3$ (see Vijayaratnam *et al.* [24]).

2.2 Peristaltic Blood Vessel

The nano-size coronavirus is propagating through peristaltic blood flow in circulatory system in the form of sinusoidal wave propagation. Mathematically the peristaltic wall motion is expressed as:

$$\bar{h}(\bar{x}, \bar{t}) = R_w - \bar{\phi} \cos^2 \frac{\pi}{\lambda} (\bar{x} - c\bar{t}). \quad (6)$$

where, \bar{h} is represented by a spatio-temporal wall function, $\bar{\phi}$ is amplitude of the wave propagation. c and λ denote the arbitrary velocity, and wave length of the channel (blood vessel), respectively.

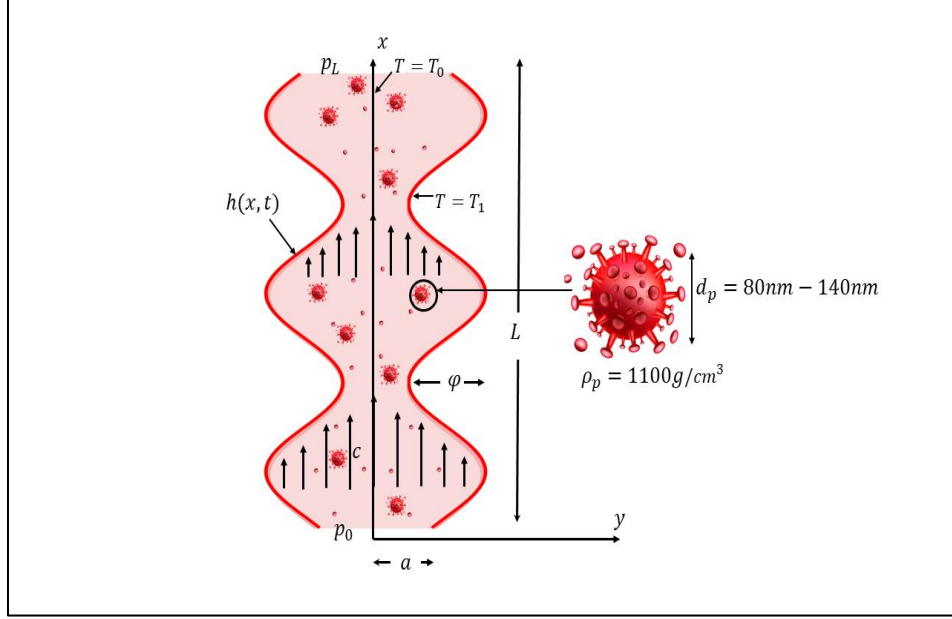


Figure 2: Schematic representation of transmission of coronavirus particle through peristaltic blood flow.

2.3 Dimensional Analysis

It is pertinent to introduce scaling parameters: $x = \frac{\pi \bar{x}}{\lambda}$, $y = \frac{\bar{y}}{R_w}$, $t = \frac{c\pi \bar{t}}{\lambda}$, $u = \frac{\bar{u}}{c}$, $v = \frac{\bar{v}}{c\varepsilon}$, $h = \frac{\bar{h}}{R_w}$, $\phi = \frac{\bar{\phi}}{R_w}$, $p = \frac{\bar{p}\varepsilon R_w}{\mu c}$. Here, x , y , t , u , v , p represent the dimensionless counterparts of the dimensional parameters. $R_w = a + \phi$ is the width of the channel, $\varepsilon = \pi \frac{R_w}{\lambda}$ is the wave number, $Re = \frac{\rho c R_w}{\mu}$ is a Reynolds number, $\nabla^2 = \varepsilon^2 \frac{\partial^2}{\partial x^2} + \frac{\partial^2}{\partial y^2}$ is the Laplacian operator, $Gr = \frac{g p \alpha R_w^2 (T_1 - T_0)}{\mu c}$ is the Grashof number, $\theta = \frac{T - T_0}{T_1 - T_0}$ is the temperature of the blood, $\beta = \frac{R_w^2 \Phi}{k(T_1 - T_0)}$ is the heat source ($\beta > 0$) or heat sink ($\beta < 0$) parameter and $Pr = \frac{\mu c p}{k}$ is the Prandtl number. The

conservation equations for the blood flow can therefore be reduced to:

$$\left(\frac{\partial u}{\partial x} + \frac{\partial v}{\partial y}\right) \frac{\varepsilon c}{Re} = 0, \quad (7)$$

$$\varepsilon Re \left(\frac{\partial}{\partial t} + u \frac{\partial}{\partial x} + v \frac{\partial}{\partial y}\right) u = -\frac{\partial p}{\partial x} + \varepsilon^2 \frac{\partial^2 u}{\partial x^2} + \frac{\partial^2 u}{\partial y^2} + Gr\theta, \quad (8)$$

$$\varepsilon^2 Re \left(\frac{\partial}{\partial t} + u \frac{\partial}{\partial x} + v \frac{\partial}{\partial y}\right) v = -\frac{\partial p}{\partial y} + \varepsilon^3 \frac{\partial^2 v}{\partial x^2} + \varepsilon \frac{\partial^2 v}{\partial y^2}, \quad (9)$$

$$\varepsilon Re Pr \left(\frac{\partial \theta}{\partial t} + u \frac{\partial \theta}{\partial x} + v \frac{\partial \theta}{\partial y}\right) = \left(\varepsilon^2 \frac{\partial \theta}{\partial x^2} + \frac{\partial^2 \theta}{\partial y^2}\right) + \beta. \quad (10)$$

Under the lubrication approximation, low Reynolds number ($Re \in [0, \varepsilon]$) and large wavelength number $\varepsilon \ll 1$ where the viscous effect is dominant, neglecting the terms of $Re \in [0, \varepsilon]$, we obtain the following version of the conservation equations:

$$\frac{\partial u}{\partial x} + \frac{\partial v}{\partial y} = 0, \quad (11)$$

$$\frac{\partial p}{\partial x} = \frac{\partial^2 u}{\partial y^2} + Gr\theta, \quad (12)$$

$$\frac{\partial p}{\partial y} = 0, \quad (13)$$

$$\frac{\partial^2 \theta}{\partial y^2} + \beta = 0 \quad (14)$$

2.4 Boundary Conditions

The boundary conditions are prescribed as follows:

$$At \quad y = 0, \partial u / \partial y = 0, \quad v = 0, \quad \partial \theta / \partial y = 0 \quad (15)$$

$$At \quad y = h, u = 0, \quad v = \frac{\partial h}{\partial t}, \quad \theta = 1 \quad (16)$$

$$At \quad x = 0, \quad p = p_0(t), \quad (17)$$

$$At \quad x = 1, \quad p = p_L(t) \quad (18)$$

2.5 Analytical Solutions

The *blood temperature* is derived as follows:

$$\theta = \frac{1}{2}(2 + \beta(h^2 - y^2)). \quad (19)$$

Axial blood velocity is obtained as:

$$u = \frac{1}{2} \frac{\partial p}{\partial x} (y^2 - h^2) - \frac{1}{24} Gr (12 + \beta(5h^2 - y^2))(y^2 - h^2). \quad (20)$$

By considering the continuity equation (6a), the *transverse blood velocity* emerges as:

$$v = \frac{1}{6}(3h^2 y - y^3) \frac{\partial^2 p}{\partial x^2} + y h \frac{\partial p}{\partial x} \frac{\partial h}{\partial x} + \frac{1}{6} y h Gr (-6 + y^2 \beta - 5\beta h^2) \frac{\partial h}{\partial x}. \quad (21)$$

As $v|_{y=h} = \partial h / \partial t$, the wall deformation rate is obtained as:

$$\frac{\partial h}{\partial t} = \frac{1}{3} \frac{\partial^2 p}{\partial x^2} h^3 + \frac{\partial p}{\partial x} \frac{\partial h}{\partial x} h^2 - \frac{\partial h}{\partial x} h^2 Gr - \frac{2}{3} \frac{\partial h}{\partial x} \beta Gr h^4. \quad (22)$$

Integrating Eqn. (22), with respect to x . the *pressure gradient* is derived as:

$$\frac{\partial p}{\partial x} = 3 \frac{1}{h^3} \int_0^x \frac{\partial h}{\partial t} dx + \frac{2}{5} \beta Gr h^2 + \frac{3}{h^3} G_0(t) + Gr. \quad (23)$$

Here $G_0(t)$ is an arbitrary function of t and derived as:

$$G_0(t) = \frac{\frac{1}{3}(\Delta p - 3 \int_0^1 (\frac{1}{h^3} \int_0^x \frac{\partial h}{\partial t} dx) dx - \frac{2}{5} \beta Gr \int_0^1 h^2 dx - Gr)}{\int_0^1 \frac{1}{h^3} dx}. \quad (24)$$

The stream function which defines the relation between the flow field and the velocity profile takes the form:

$$\psi = \frac{1}{120} (y - h)^2 (20 \frac{\partial p}{\partial x} (y + 2h) + Gr(y(-20 + y^2 \beta) - h(40 - 2y^2 \beta + \beta h(7y + 16h))))). \quad (25)$$

3 RESULTS AND DISCUSSION

3.1 Blood velocity profiles and streamlines

In this section, the velocity vectors and flow field behavior corresponding to peristaltic blood flow in the channel (blood vessel) are addressed. The particles are allowed to propagate in the fluid under the influence of Stokes force and constant gravitational field. Typically, the diameter of the blood vessel is within the range of $1 - 20 \mu m$, as referred in Tu *et al.* [25]. The velocity of the fluid particle in the blood vessel varies from approximately $1 mm/s$ to $50 cm/s$ [26, 27]. **Fig. 3** represents the blood velocity vector pattern inside the channel with $\phi = 0.4$ and $t = 0.1$. In the numerical computations, two cases are analyzed, (a) $Gr = 0$, $\beta = 0$ i.e., without thermal effects and (b) $Gr = 1$, $\beta = 2$, with thermal effects. Here, a stagnation line is present at the centre which bifurcates the velocity vector at the relaxation region. On the other hand, the propagative flow field acts at the contraction region, which propels the physiological fluid in the upward (forward) direction. This mechanism controls the blood flow in the vessel. In addition, the impacts of buoyance force (i.e., Grashof number (Gr)) and heat source ($\beta > 0$) on streamlines of the velocity vector $U_i = (u, v, 0)$ are illustrated through **Figs. 3(a & b)**. From these figures, it is observed that both parameters are responsible for the smooth and high velocity in the blood vessel (i.e., when body temperature rises, blood flow inside the circulatory system increases). **Figs. 4 (a & b)** show the stream function contours of the $u-v$ vector and in excess of a five fold boost in magnitudes is

observed from the non-thermal case (a) $Gr = 0$, $\beta = 0$ to the thermal case b) $Gr = 1$ and $\beta = 2$. In particular, there is a strong alignment in streamlines along the central (core) channel zone, indicating the flow is intensified in the vessel with heat source and thermal buoyancy forces. Effectively therefore the presence of heat transfer (natural convection) and heat generation, which characterizes real blood flows, encourages acceleration in the vessel.

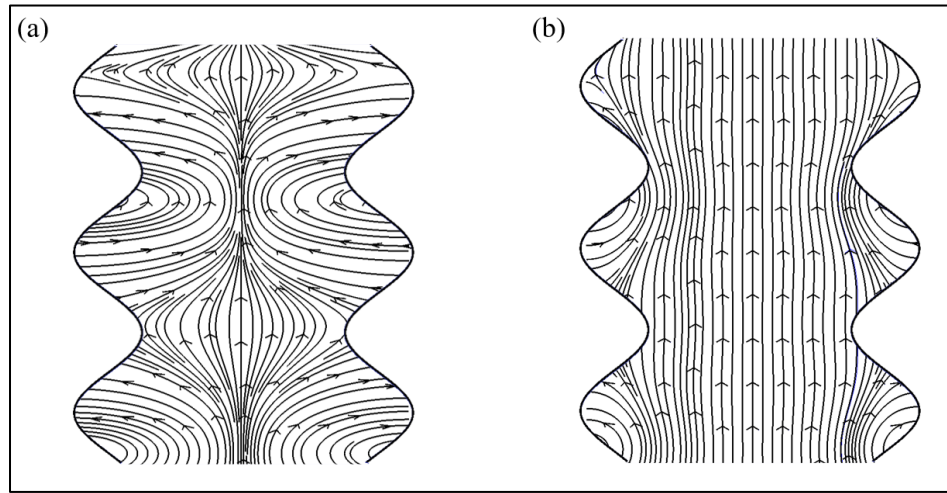


Figure 3: Streamlines of the blood velocity vectors for (a) $Gr = 0$, $\beta = 0$ (b) $Gr = 1$, $\beta = 2$.

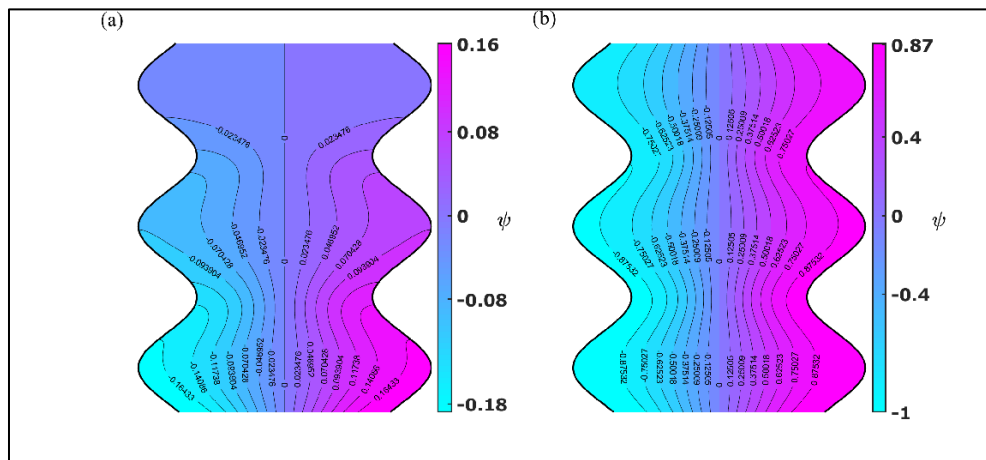


Figure 4: Contour of the stream function for (a) $Gr = 0$, $\beta = 0$ (b) $Gr = 1$, $\beta = 2$.

3.2 Virus Transport in Peristaltic Blood Flow

The transport of a small size virion in the blood vessel can be described by the Boussinesq-Basset

equation. This equation expresses the transient hydrodynamic force which helps to correlate the motion of the nano-size particles subject to uniform/non-uniform flow in the circulatory system and it is mathematically expressed as:

$$\begin{aligned} \frac{m_p d\bar{v}_i}{d\bar{t}} &= (m_p - m)\bar{g} + m_f \frac{D\bar{U}_i}{D\bar{t}} - \frac{1}{2}m\bar{V}_i - \bar{U}_i - 6\pi r\mu\bar{V}_i - \bar{U}_i \\ &- 6\pi r^2\mu \left(\int_0^{\bar{t}} \frac{\left(\frac{d}{dt}(\bar{v}_i - \bar{U}_i)\right)}{\sqrt{(\pi v(\bar{t} - \tau))}} d\tau + \frac{(v_{i0} - U_{i0})}{\sqrt{\bar{t}}} \right). \end{aligned} \quad (26)$$

Here $r = \frac{d_p}{2}$ is the particle radius (d_p is the particle diameter). Jiménez-Lozano *et al.* [27] have shown that the influence of drag force contributes more significantly the particles motion in fluid medium for example, micro-size bacteria particles in the ureter, rather than all the other forces acting on the particle motion. Kim *et al.* [28] have noted that if the density of the particle is lower than fluid density, then several fluid forces such as buoyancy force, Basset force, pressure force and Faxen corrections (wherein Stokes drag force acting on a particle is increased due to the presence of a neighboring wall) may affect the particle motion. The following dimensionless quantities are implemented in Eq. (26) to utilize suitable assumptions:

$$\begin{aligned} u_p &= \frac{\bar{u}_p}{c}, \quad v_p = \frac{\bar{v}_p}{c}, \quad g = \frac{\bar{g}}{g_0}, \quad \tau_c = \frac{\lambda}{\pi c}, \quad \tau_p = \frac{\rho_p d_p^2}{18\mu}, \\ \alpha &= \frac{d_p}{R_w}, \quad S_N = \frac{\tau_p}{\tau_c}, \quad S = \rho_p / \rho_f. \end{aligned} \quad (27)$$

Here, the convective acceleration (Stokes flow) approximating the substantial derivative $\left(\frac{D}{Dt}\right)$ as $\left(\frac{d}{dt}\right)$ is exact to the order of approximation required for uniform blood flows. The Boussinesq-Basset equation can now be written as:

$$\begin{aligned} \frac{dv_i}{dt} &= \frac{1}{S_N} \left(\frac{2S}{2S+1} \right) (V_i - U_i) + \frac{3}{2S+1} \frac{dU_i}{dt} \\ &+ \sqrt{\frac{9}{2\pi S S_N}} \left(\frac{2S}{2S+1} \right) \left(\int_0^{\bar{t}} \frac{\left(\frac{d}{dt}(v_i - U_i)\right)}{\sqrt{\bar{t} - \tau}} d\tau + \frac{(v_{i0} - U_{i0})}{\sqrt{\bar{t}}} \right) \\ &+ \frac{2(S-1)}{2S+1} \frac{\tau_c}{c} g_0 g. \end{aligned} \quad (28)$$

The *axial and transverse* components of the particle (virus) velocity vector are expressed as:

$$\begin{aligned} \frac{du_p}{dt} &= \beta_1(u - u_p) + \beta_2 \frac{du}{dt} + \\ &\beta_3 \left(\int_0^t \frac{\left(\frac{d}{dt}(u - u_p)\right)}{\sqrt{t - \tau}} d\tau + \frac{(u_0 - u_{p0})}{\sqrt{t}} \right), \end{aligned} \quad (29)$$

$$\begin{aligned} \frac{dv_p}{dt} &= \beta_1(v - v_p) + \beta_2 \frac{dv}{dt} + \\ &\beta_3 \left(\int_0^t \frac{\left(\frac{d}{dt}(v-v_p) \right)}{\sqrt{t-\tau}} d\tau + \frac{(v_0-v_{p0})}{\sqrt{t}} \right) - \beta_4. \end{aligned} \quad (30)$$

Here:

$$\begin{aligned} \beta_1 &= \frac{1}{S_N} \left(\frac{2S}{2S+1} \right), \beta_2 = \frac{3}{2S+1}, \beta_3 = \sqrt{\frac{9}{2\pi S S_N}} \left(\frac{2S}{2S+1} \right), \\ \beta_4 &= \frac{2(S-1)}{2S+1} \frac{\tau_c}{c} g_0 g \end{aligned} \quad (31)$$

In the present theoretical study of virus transmission in peristaltic blood flow, it is of interest to analyse also the effect of fluid temperature on the transmission of virus. In this respect, *axial and transverse velocity components of the virus* are derived as the solutions of Eqns. 29 and 30 subject to boundary condition $u_p|_{t=0} = 0$, and $v_p|_{t=0} = 0$, as follows:

$$u_p = I_0 \int_0^t I_1 \left(\beta_1 u + \beta_2 \frac{du}{dt} + 1.41\beta_3 \frac{u}{\sqrt{t}} \right) dt \quad (32)$$

$$v_p = I_0 \int_0^t I_1 \left(\beta_1 v + \beta_2 \frac{dv}{dt} + 1.41\beta_3 \frac{v}{\sqrt{t}} - \beta_4 \right) dt \quad (33)$$

where $I_0 = e^{-\beta_1 t} e^{-2.82\beta_5 \sqrt{t}}$. and $I_1 = e^{\beta_1 t} e^{2.82\beta_5 \sqrt{t}}$.

3.3 Parameter selection

Based on the data available in the literature [26] the appropriate clinical parametric details selected for the virus and blood, and further computed other parameters' values/ranges for the simulation of virus movement through peristaltic blood flow and tabulated in **Tables 1 and 2** respectively.

Table 1: Parametric values of circulatory system (blood stream)

Parameters Definition	Wavelength (λ ; mm)	Wave velocity (c ; mm/sec)	Blood density (ρ ; kg/m ³)	Gravity (g_0 ; m/sec ²)	Fluid (blood) characteristic time ($\tau_c = \frac{\lambda}{\pi c}$)
Point Estm.	120	300-400	1060	1	0.127

Table 2: Estimates of parameters associated with novel Coronavirus SARS COV-2 at the average density ρ_p of virus in blood stream 1100kg/m³

Parameter Definition	Formula	Parametric Range of blood viscosity & virus diameter
		Blood viscosity (μ): 3.3×10^{-3} Ns/m ² Virus diameter (d_p): 80-140 nm
The particle relaxation time (τ_p)	$\frac{\rho_p d_p^2}{18\mu}$	$(1.185 - 3.629) \times 10^{-10}$
Stokes number (S_N)	τ_p/τ_c	$(0.933 - 2.857) \times 10^{-9}$
Density ratio (S)	ρ_p/ρ	1.037
Drag force (β_1)	$\frac{1}{S_N} \left(\frac{2S}{2S+1} \right)$	$(7.231 - 2.361) \times 10^8$
Virtual mass force (β_2)	$\frac{3}{2S+1}$	0.976
Basset (β_5)	$\sqrt{\frac{9}{2\pi S S_N}} \left(\frac{2S}{2S+1} \right)$	$(2.596 - 1.483) \times 10^4$
Gravity (β_6)	$\frac{2(S-1)}{2S+1} \frac{\tau_c}{c} g_0 g$	0.099

From **Table 2**, the average values of (β_1): 3.56×10^8 and $\beta_5 = 1.822 \times 10^4$ are considered for the computation of the results.

3.4 Transmission of SARS-CoV-2 by droplet particle packing

This has been a matter of discussion whether the virus can transmit by air or not. Some studies report that virus spread is reduced as the size of the microdroplet particle is increased see [16, 29]. Thomas [30] has reported that the range of the microdroplet particle is $1\mu m$ (even smaller) to 2mm. Many studies reported that the microdroplet particles $< 5\mu m$ constitute an aerosol. On the other hand, Mathews *et al.* [31] have demonstrated that the microdroplet particle contains the minimum amount of gel form as compared to the contribution of virions which make them solid aerosols. In this regard, Nor *et al.* [32] have noted that a virus can be transported via solid aerosols. Furthermore, it is important to know that how many virions of SARS-CoV-2 transmit from an infected person to non-infected person, which helps to protect the vulnerable and control the spread

of the SARS-CoV-2 infection. **Fig. 5** shows the mechanism of transmission of virion infection from an infected person to a non-infected person. During the interaction, the virion droplet which resides in the infected person (red head) is transferred to another person (green head) via human activity including coughing, talking, laughing, sneezing etc.

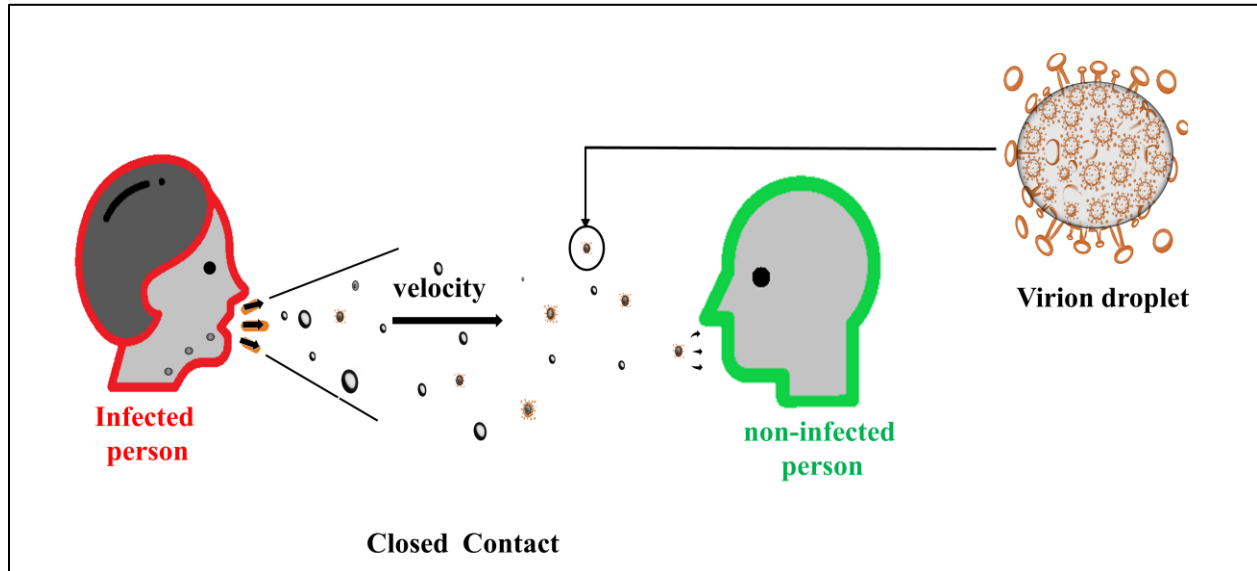


Figure 5: An illustration of transmission of virion infection from an infected person to a non-infected person.

In this study, Kepler conjecture is deployed which provides a theorem for the optimal packaging of virions in a droplet particle. Following Hales [33], the Kepler approach considers that the density of compact packing arrangements is around $\pi/\sqrt{18} = 74.048$. Since, coronavirus particles are assumed to possess a spherical shape, the possible amount of virions of diameter $d_p = 80 - 140 \text{ nm}$ that can be packaged in a droplet diameter $D_p = 2 - 100 \text{ }\mu\text{m}$ (consider) is defined as follows:

$$N_p = 74.048 \frac{\text{volume of the droplet}}{\text{volume of the particle}} \quad (34)$$

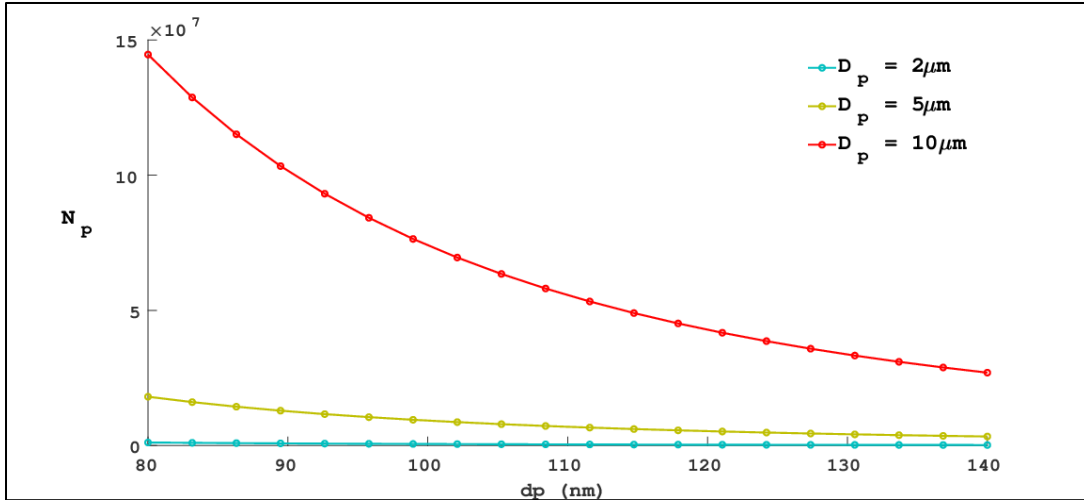


Figure 6: Number of virions (N_p) with SARS-CoV-2 diameter d_p (nm) for different droplet diameters.

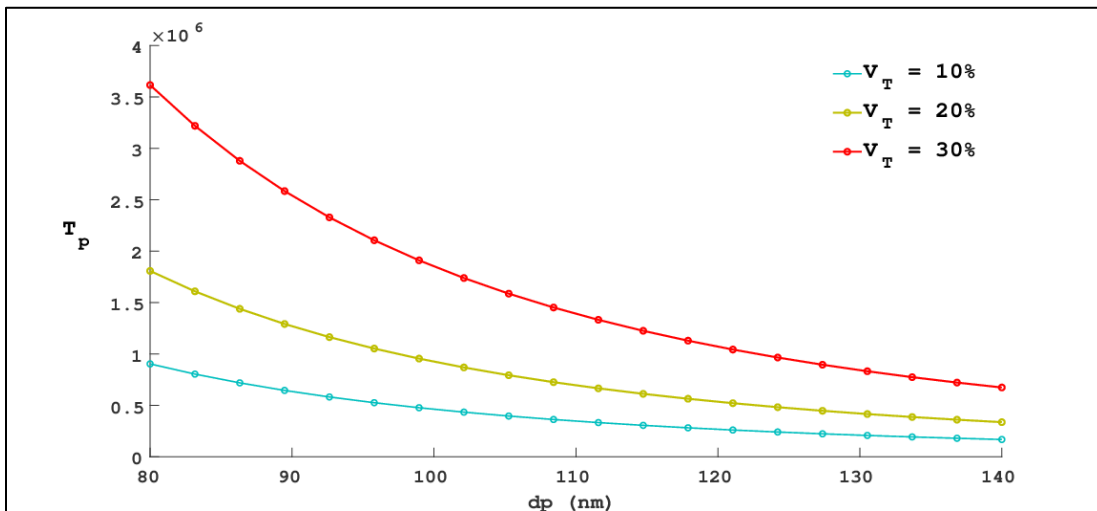


Figure 7: Number of transmission virions (T_p) with SARS-CoV-2 diameter d_p (nm) for different virion transmission percentage (V_T).

Thus far, the distinction between the size of microdroplet particles (i.e., either aerosol or droplet) has been discussed. A key question is *whether aerosol particles are responsible for the infection transmission from person to person?* As noted by Thomas [30], the majority of SARS-CoV-2 virions which reside in the respiratory tract of an infected person (i.e., less than $10 \mu\text{m}$ the droplet) is 78-96% in the form of microdroplets, while only 4-46% of virus particles are produced during coughing and sneezing. From **Fig. 6**, it is observed that the nano-size SARS-CoV-2 virus particle

can reside inside the microdroplet of an infected person. Here, the number of SARS-CoV-2 virions is 10^6 in the droplet of diameter $2\mu m$, while 10^7 virions are reported for the droplet of diameter $10\mu m$. This result shows that as the microdroplet size is decreased, they carry less quantities of coronavirus particles that is why an airborne infection is less harmful, which has also been documented by Smith [16] and Santa-Coloma [34]. The transmission of SARS-CoV-2 virus particles from one infected person to non-infected person is illustrated in **Fig. 7**. The transmission of virus particles depends on the oral and nasal activity of the human (such as breathing, talking, laughing, coughing, sneezing, etc.). In the context of human activity, we have considered three possibilities of virion transmission (such as 10%, 20%, 30%) during the coughing and sneezing in the droplet of diameter $5\mu m$. The magnitude of the number of SARS-CoV-2 virions is 10^6 in the aerosol particle ($5\mu m$). If the percentage of transmission of the aerosol particle is less with a low viral load (the amount of virion makes a person sick), there is no much impact of infection to another person. However, if the viral load is high or the transmission percentage is large, the non-infected person may be infected.

3.5 Estimate of infection transmission through blood flow

It has been noticed that the transmission of infection from person to person through coughing, talking, laughing and sneezing mainly depends on the density and initial velocity of the virion droplet from the nasal zone or mouth. Initially, some smaller size virions are rapidly evaporated due to the humidity and temperature of the local environment, as elaborated earlier by Galton *et al.* [35] and Fernstrom and Goldblatt [36]. The remaining virions either travel in the air or fall to the ground depending on the size and density of the microdroplet. During the process of inhalation, some aerosol particles avoid getting trapped in the mucus and cilia, and they are deposited in the bronchoalveolar region of the lungs, liver, heart, and stomach. The virions entering the body mainly depend on the droplet characteristics such as droplet size, droplet velocity, temperature, type of pathogen, the activity of pathogen, etc. Among these parameters, we have considered the blood vessel as a pathway via peristaltic motion that transports the blood containing virus in the circulatory system. Once the SARS-CoV-2 virus (droplets) have entered the circulatory system through the nose or mouth, some time is required before they settle within the bloodstream.

Fig. 8 illustrates the variation of the virion particle relaxation time with SARS-CoV-2 virion diameter for different blood viscosity. This figure shows that the small size virus particle ($d_p =$

80nm) rapidly settles inside the bloodstream as compared to large size virus particles ($d_p = 140nm$). Further, it is observed that the virions take more time to settle in blood with lower viscosity. This would indicate that the infection period time is less for lower viscosity blood.

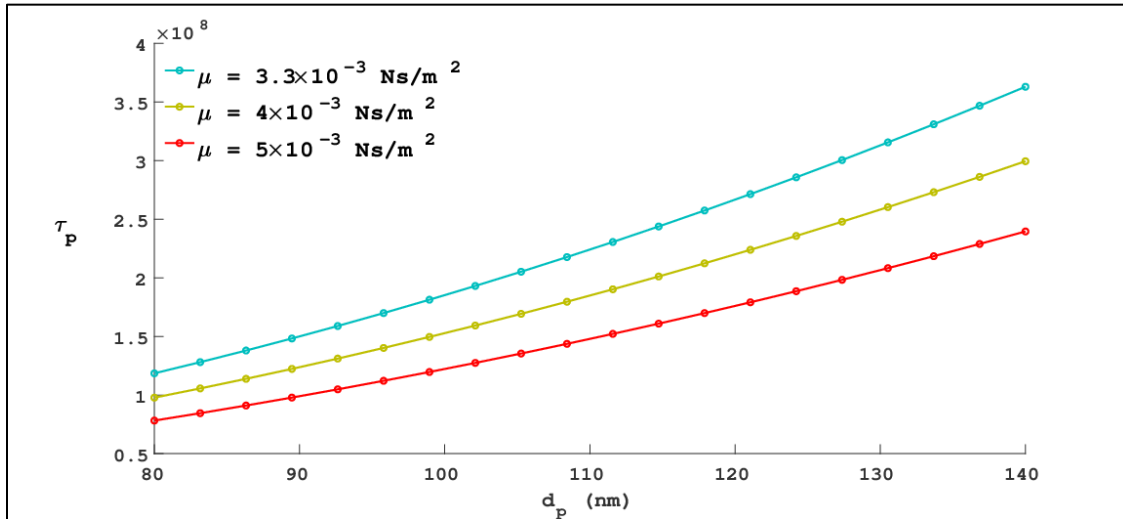


Figure 8: The variation in the particle relaxation time with particle diameter at a fixed value of $\phi = 0.4$, and $x = 0.3$.

3.6 Thermal effects on the transmission of SARS-CoV-2 through blood flow

Using the mathematical model described earlier, it has been possible to analyse the progression of SARS-CoV-2 through a blood vessel. Additionally, the effect of temperature and applicable forces on the transmission of SARS-CoV-2 has been computed. In this mathematical model, parameters such as diameter and density of the virus particle, and viscosity of the blood have been considered to achieve more accurate results as presented in **Table 1**. From the literature, it is observed that peristaltic pumping mechanism transports the nanosize particles/molecules along the direction of blood flow within the velocity range of 300-400 *mm/sec* in humans.

Fig. 9 illustrates that how the SARS-CoV-2 virus particle moves through blood flow. Since the axial velocity of the fluid is zero at the wall of the blood vessel (due to the consideration of no-slip boundary condition), the particle axial velocity is also zero which validates our result. The wave-like progression of the virion velocity is influenced naturally via the peristaltic (contraction and relaxation of blood vessels) movement of the blood in circulatory system. The axial virion attains high velocity (of the order of multiples of 10^7) in the blood vessel. In other words, once the virus

particle enters into the physiological systems it will rapidly move along with the bloodstream and spread throughout the cardiovascular system. Typically, body temperature exerts a key role in influencing blood flow in the circulatory system. Further blood absorbs and distributes heat throughout the physiological system. When bacteria/viruses enter inside the body, the blood vessels react rapidly via expansion and contraction of the vessels. The actuation of the blood vessel transports the blood and heat (thermal energy) to other locations, wherever it is required. Consequently, the axial velocity of the particle is slightly increased with heat generation (source) ($\beta = 5$) as shown in **Fig. 9**. From the physical point of view, the closed packed structure of the virions is loosened in the blood vessel due to the more temperature of the blood. Therefore, the arrangement of packing densities will decrease, and they will be separated from each other, resulting in a reduction in the innervation of tissues and blood vessels. Further, the viscosity of the blood becomes reduced as $\mu = (2(\rho_p - \rho) * g * a^2)/(9 * v)$ and hence blood circulation is improved, which further amplifies virion transport in the system.

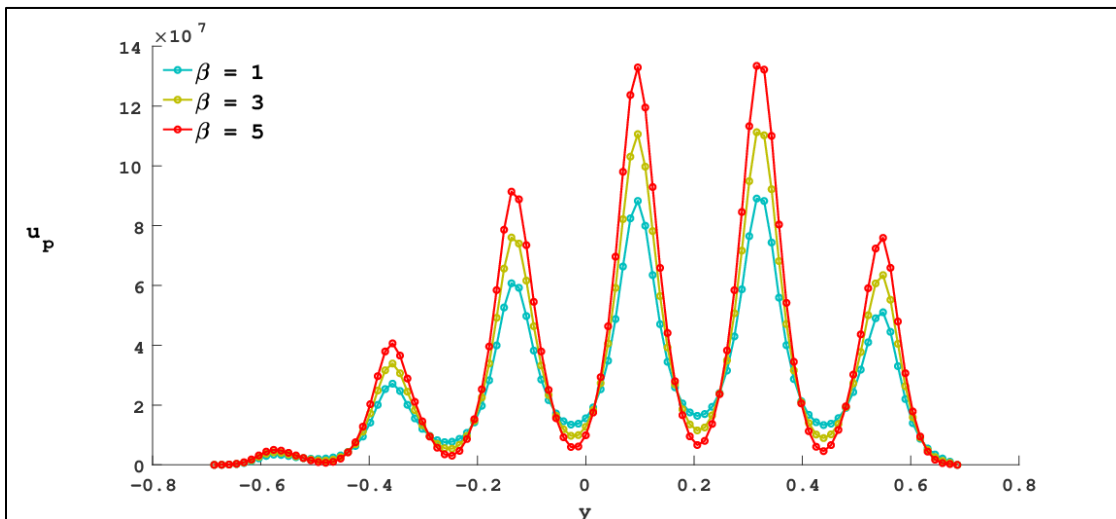


Figure 9: The variation in the axial virus velocity for different values of heat source parameter (β) at a fixed value of $\phi = 0.4, t = 0.4$ & $x = 0.2$.

Figure 10 illustrates the impact of thermal buoyancy force on the motion of the virion. Grashof number (Gr) is the ratio of the buoyancy force to viscous force. Earlier, we discussed that if the particle density is less than the fluid density, the dynamics of particle flow becomes complex. The buoyancy force is one of the fluid forces that can affect the motion of the virus when the fluid density is greater than the particle density. From **Fig. 10**, it is observed that the Gr is responsible

for the large axial velocity of the virion i.e., SARS-CoV-2 particle is strongly influenced via the upthrust associated with free convection currents. It will remain suspended continuously and take time to settle at the body surface /tissues so that it will take time to damage the tissues (internal organs). The case $Gr = 0$ corresponds to forced convection for which thermal buoyancy is absent. Further, the transient behaviour of axial velocity of the virus particle at fixed position $x = 0.3$ is displayed in **Fig. 11** with the effect of heat generation (β). The profiles computed show that the particle behavior is almost uniform throughout time. With increasing heat source parameter, thermal effect is increased and axial particle velocity is slightly increased, but only after a critical time elapse. In addition, we observed that the velocity of the SARS-CoV-2 particle is of the order of 10^5 and therefore significantly lower than the spatial velocity distribution shown earlier in **Fig. 9**. From this result, it is concluded that the virion velocity is non-uniform throughout the blood vessel due to sinusoidal rhythmic contraction and expansion of the moving walls, while at a fixed position the virion velocity is constant.

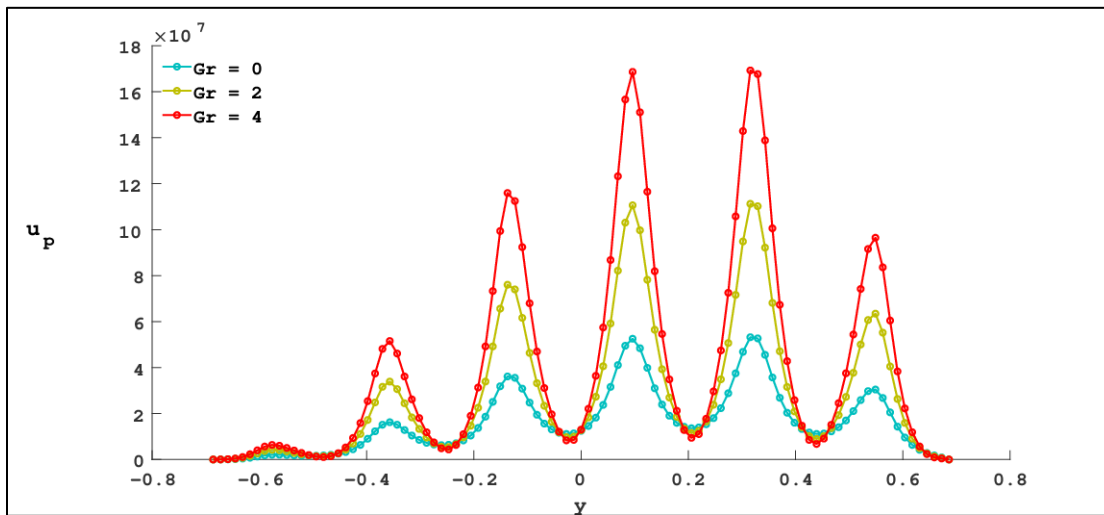


Figure 10: The variation in the axial virus velocity for different values of Grashof number at fixed value of $\phi = 0.4, t = 0.4$ & $x = 0.2$.

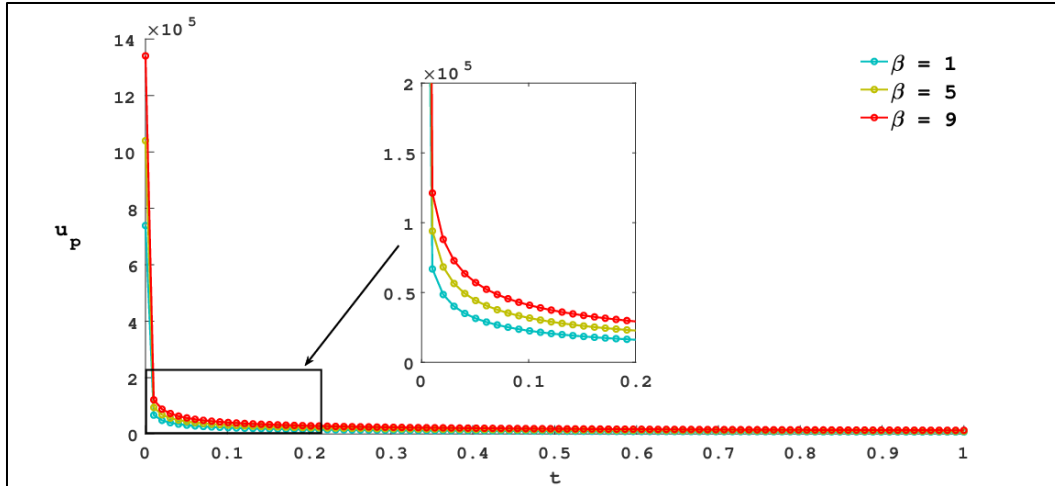


Figure 11: The variation in the axial particle velocity of the virus particle with time at fixed values of $\phi = 0.4, t = 0.4$ & $x = 0.2$.

Figures 12 & 13 illustrate respectively the streamlines of the axial virion velocity and flow field of the virion for different values of the buoyance force (Gr) and heat source (β) parameters. From the literature survey, it is observed that the extent of virus enveloping fluid droplets is reduced with diameter due to humidity and temperature impact. Further, the virus can remain in the air for extended periods of time. Mecenas *et al.* [3] considered the case where the droplet size is small due to the removal of liquid contents in the envelope and observed that the virus is expelled at higher temperature but that this is a slow process. With this in mind, the streamlines of the axial velocity of the virus particle may help to understand the phenomena associated with SARS-CoV-2 virus flow in a blood vessel. The axial velocity of the virion in the absence of heat generation and thermal buoyancy ($\beta=Gr=0$) is observed to decrease as depicted in **Fig. 12(a)**. However, the stream lines of the virion axial velocity are intensified with heat generation and thermal buoyancy both as shown in **Fig. 12(b)**. The evaporation of liquid contents from the droplets reduces the diameter of enveloped viruses and their density due to high temperature. Therefore, reduction of virion droplet size and thermal buoyancy force uplifting the droplet increases the velocity magnitude. Corresponding to the virion axial velocity, **Fig. 13** represents the movement of the virus particle in the blood vessel. From this result, it is evident that that the virion takes time to be activated with greater thermal effects depending on the environment and body temperature. Temperature can reduce the virion influence but will not completely expel the virion. Since the water density is $1000\text{Kg}/\text{m}^3$ which evaporates at 100°C , however, the SARS-CoV-2 virion density of 1100kg , will modify the overall evaporation temperature of the infected blood. Since

normal human body temperature is around 37.5°C , this is insufficient to expel the SARS-CoV-2 virus; however higher temperatures can mitigate to some extent the transmission of virus particles in blood flow.

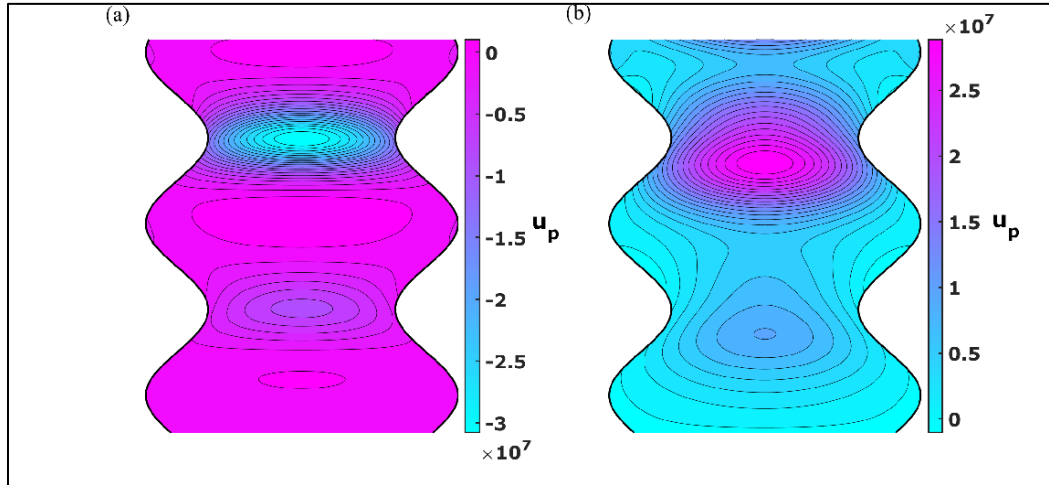


Figure 12: The streamlines for axial movement of SARS-CoV-2 virus in the blood vessel for (a) no impact of buoyancy force and heat source (b) the appearance of buoyancy force ($Gr = 2$) and heat source ($\beta = 5$) at fixed values of $\phi = 0.4, t = 0.4$ & $x = 0.2$.

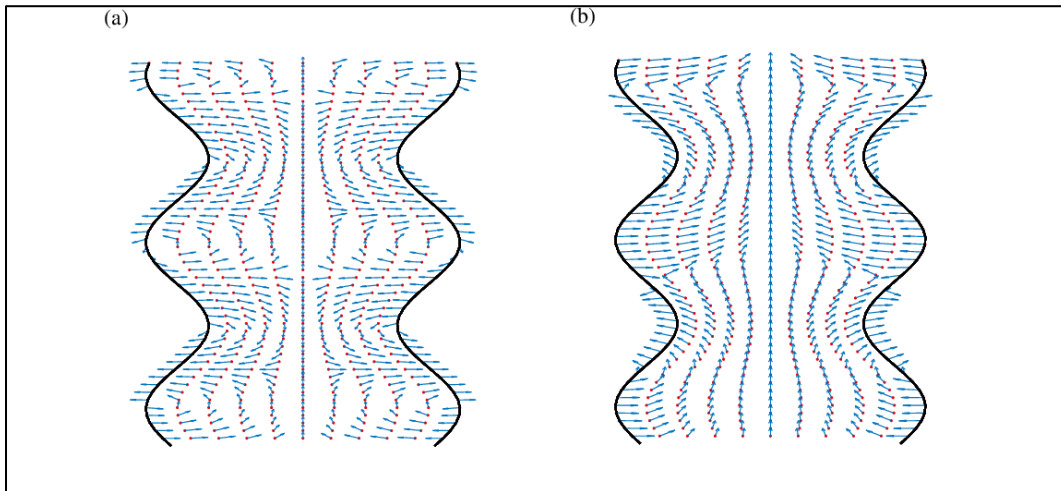


Figure 13: The flow field of SARS-CoV-2 virus in the blood vessel for (a) no impact of buoyancy force and heat source (b) the appearance of buoyancy force ($Gr = 2$) and heat source ($\beta = 5$) at fixed values of $\phi = 0.4, t = 0.4$ & $x = 0.2$.

4 Conclusions

A mathematical study of the the transient motion of coronavirus particles through blood flow driven by peristaltic pumping, has been presented. Thermal buoyancy and heat generation effects are analyzed. The modelling deployed assumes that coronavirus particles with a diameter of $120\mu m$ and a density of $1g/cm^3$ move in the direction of blood flow. The quantity of SARS-CoV-2 virions (entire virus particles) inside a microdroplet is calculated by considering the Kepler conjecture method and the transmission percentage of viral load is also computed. Computations are performed to visualize the streamline profiles, variation in the particle relaxation time with particle diameter, distribution of number of virions (N_p) with SARS-CoV-2 diameter $d_p(nm)$ for different particle diameters and also the evolution of transmission virions (T_p) with SARS-CoV-2 diameter $d_p(nm)$ for different virion transmission percentage (V_T). Considering that there is no physical barrier preventing viruses inside the microdroplets, some of the key findings are summarized as:

- During the interaction, the air route of infection is possible through the infected person to non-infected person via human activities including coughing, talking, laughing, and sneezing.
- If the percentage of transmission of the SARS-CoV-2 virion is less with a low viral load (the amount of virion that makes a person sick), there are fewer chances to infect another person.
- The small size virus particle ($d_p = 80nm$) rapidly settles inside the bloodstream as compared to large size virus particles ($d_p = 140nm$).
- The virus particles can be expelled in humans depending on their anatomy such as body temperature, lung capacity, surface properties of the lung airways, etc. [23]. However, if the SARS-CoV-2 particle remains inside the body for a long time, it can cause damage to blood vessels and tissues.
- The evaporation of liquid contents from the droplets reduces the diameter of enveloped viruses and their density due to high temperature.
- Temperature plays a significant role in reducing the package density of the virion droplet i.e., the cohesion of the particles is reduced with an increment in temperature so that the SARS-CoV-2 takes greater time to affect the body.

The present investigation may assist in providing deeper insights to medical researchers related to how SARS-CoV-2 virus particles spread through blood flow and what will be the significant role of thermal effects, and furthermore infection SARS-CoV-2 in physiological systems. In the present work, attention has been confined to Newtonian fluid model for blood however the future investigations may present with non-Newtonian rheological properties of blood.

Author's Contributions

Dharmendra Tripathi: Conceptualization, Methodology, Editing, Revision, Supervision

Dinesh Singh Bhandari: Derivation, Computation, Writing –original draft, and Revision,

O. Anwar Béq: Editing, analysis, and Revision.

Data Availability

The data that supports the findings of this study are available within the article.

Conflict of interest

The authors declare that they have no conflict of interest.

Declaration of competing interest

The authors declare that they have no known competing financial interests or personal relationships that could have appeared to influence the work reported in this paper

Acknowledgements

The authors are grateful to all the reviewers for their excellent comments which have served to improve the paper.

References

1. DM Berry and June D Almeida. The morphological and biological effects of various antisera on avian infectious bronchitis virus. *Journal of General Virology*, 3(1):97–102, 1968.
2. Raymond Tellier. Review of aerosol transmission of influenza a virus. *Emerging Infectious Diseases*, 12(11):1657, 2006.
3. Paulo Mecnas, Renata Travassos da Rosa Moreira Bastos, Antonio Carlos Rosário Vallinoto, and David Normando. Effects of temperature and humidity on the spread of covid-19: A systematic review. *PLoS One*, 15(9):e0238339, 2020.
4. Santosh K Das, Jan-e Alam, Salvatore Plumari, and Vincenzo Greco. Airborne virus

- transmission under different weather conditions. *AIP Advances*, 12(1):015019, 2022.
5. Syed Emdadul Haque and Mosiur Rahman. Association between temperature, humidity, and covid-19 outbreaks in bangladesh. *Environmental Science & Policy*, 114:253–255, 2020.
 6. Patrick CY Woo, Susanna KP Lau, Chung-ming Chu, Kwok-hung Chan, Hoi-wah Tsoi, Yi Huang, Beatrice HL Wong, Rosana WS Poon, James J Cai, Wei-kwang Luk, et al. Characterization and complete genome sequence of a novel coronavirus, coronavirus hku1, from patients with pneumonia. *Journal of Virology*, 79(2):884–895, 2005.
 7. Martin R Maxey and James J Riley. Equation of motion for a small rigid sphere in a nonuniform flow. *Physics of Fluids*, 26(4):883–889, 1983.
 8. MM Bhatti, A Zeeshan, M Aleem Asif, R Ellahi, and Sadiq M Sait. Non-uniform pumping flow model for the couple stress particle-fluid under magnetic effects. *Chemical Engineering Communications*, pages 1–12, 2021.
 9. Bhatti, Muhammad Mubashir, and Sara I. Abdelsalam. "Thermodynamic entropy of a magnetized Ree-Eyring particle-fluid motion with irreversibility process: a mathematical paradigm." *ZAMM-Journal of Applied Mathematics and Mechanics/Zeitschrift für Angewandte Mathematik und Mechanik* 101, no. 6 (2021): e202000186.
 10. MM Bhatti, A Zeeshan, F Bashir, Sadiq M Sait, and Rahamat Ellahi. Sinusoidal motion of small particles through a Darcy-Brinkman-Forchheimer microchannel filled with non-newtonian fluid under electro-osmotic forces. *Journal of Taibah University for Science*, 15(1):514–529, 2021.
 11. Ji-Xiang Wang, Yun-Yun Li, Xiang-Dong Liu, and Xiang Cao. Virus transmission from urinals. *Physics of Fluids*, 32(8):081703, 2020.
 12. Mohammad S Islam, Puchanee Larpruenrudee, Akshoy Ranjan Paul, Gunther Paul, Tevfik Gemci, Yuantong Gu, and Suvash C Saha. Sars cov-2 aerosol: How far it can travel to the lower airways? *Physics of Fluids*, 33(6):061903, 2021.
 13. Mohammad S Islam, Puchanee Larpruenrudee, Suvash C Saha, Oveis Pourmehran, Akshoy Ranjan Paul, Tevfik Gemci, Richard Collins, Gunther Paul, and Yuantong Gu. How severe acute respiratory syndrome coronavirus-2 aerosol propagates through the age-specific upper airways. *Physics of Fluids*, 33(8):081911, 2021.
 14. Warren H Finlay. *The Mechanics of Inhaled Pharmaceutical Aerosols: An Introduction*. Academic press, 2001.

15. W Holländer and SK Zaripov. Hydrodynamically interacting droplets at small Reynolds numbers. *International Journal of Multiphase Flow*, 31(1):53–68, 2005.
16. Scott H Smith, G Aernout Somsen, Cees Van Rijn, Stefan Kooij, Lia Van Der Hoek, Reinout A Bem, and Daniel Bonn. Aerosol persistence in relation to possible transmission of sars-cov-2. *Physics of Fluids*, 32(10):107108, 2020.
17. Kiril P Selverov and Howard A Stone. Peristaltically driven channel flows with applications toward micromixing. *Physics of Fluids*, 13(7):1837–1859, 2001.
18. Ali, N., S. Hussain, and K. Ullah. "Theoretical analysis of two-layered electro-osmotic peristaltic flow of FENE-P fluid in an axisymmetric tube." *Physics of Fluids* 32, no. 2 (2020): 023105.
19. Ali, Nasir, Kaleem Ullah, and Husnain Rasool. "Bifurcation analysis for a two-dimensional peristaltic driven flow of power-law fluid in asymmetric channel." *Physics of Fluids* 32, no. 7 (2020): 073104.
20. Alokaily, Samer, Kathleen Feigl, and Franz X. Tanner. "Characterization of peristaltic flow during the mixing process in a model human stomach." *Physics of Fluids* 31, no. 10 (2019): 103105.
21. Ashtari, O., M. Pourjafar-Chelikdani, K. Gharali, and K. Sadeghy. "Peristaltic transport of elliptic particles: A numerical study." *Physics of Fluids* 34, no. 2 (2022): 023314.
22. Aditya Bandopadhyay, Dharmendra Tripathi, and Suman Chakraborty. Electroosmosis-modulated peristaltic transport in microfluidic channels. *Physics of Fluids*, 28(5): 052002, 2016.
23. Jiahui Chen, Kaifu Gao, Rui Wang, Duc Duy Nguyen, and Guo-Wei Wei. Review of covid-19 antibody therapies. *Annual Review of Biophysics*, 50:1–30, 2021.
24. Pujith RS Vijayaratnam, Caroline C Oâ€™Brien, John A Reizes, Tracie J Barber, and Elazer R Edelman. The impact of blood rheology on drug transport in stented arteries: steady simulations. *PloS One*, 10(6):e0128178, 2015.
25. Tse-Yi Tu and Paul C-P Chao. Continuous blood pressure measurement based on a neural network scheme applied with a cuffless sensor. *Microsystem Technologies*, 24(11):4539–4549, 2018.
26. H Minasyan. Bactericidal capacity of erythrocytes in human cardiovascular system. *Int Clin Pathol J*, 2(5):00052, 2016.

27. Joel Jiménez-Lozano, Mihir Sen, and Patrick F Dunn. Particle motion in unsteady two-dimensional peristaltic flow with application to the ureter. *Physical Review E*, 79(4): 041901, 2009.
28. Inchul Kim, Said Elghobashi, and William A Sirignano. On the equation for spherical-particle motion: effect of reynolds and acceleration numbers. *Journal of Fluid Mechanics*, 367:221–253, 1998
29. Alibek Issakhov, Yeldos Zhandaulet, Perizat Omarova, Aidana Alimbek, Aliya Borsikbayeva, and Ardak Mustafayeva. A numerical assessment of social distancing of preventing airborne transmission of covid-19 during different breathing and coughing processes. *Scientific Reports*, 11(1):1–39, 2021.
30. Richard James Thomas. Particle size and pathogenicity in the respiratory tract. *Virulence*, 4(8):847–858, 2013.
31. Santhosh Samuel Mathews. A computer simulation study on novel corona virus transmission among the people in a queue. *medRxiv*, 2020.
32. Norefrina Shafinaz Md Nor, Chee Wai Yip, Nazlina Ibrahim, Mohd Hasni Jaafar, Zetti Zainol Rashid, Norlaila Mustafa, Haris Hafizal Abd Hamid, Kuhan Chandru, Mohd Talib Latif, Phei Er Saw, et al. Particulate matter (pm_{2.5}) as a potential sars-cov-2 carrier. *Scientific Reports*, 11(1):1–6, 2021.
33. Thomas C Hales. The sphere packing problem. *Journal of Computational and Applied Mathematics*, 44(1):41–76, 1992.
34. Tomás Santa-Coloma. The airborne and gastrointestinal coronavirus sars-cov-2 pathways. 2020.
35. Jan Gralton, Euan Tovey, Mary-Louise McLaws, and William D Rawlinson. The role of particle size in aerosolised pathogen transmission: a review. *Journal of Infection*, 62(1):1–13, 2011.
36. Aaron Fernstrom and Michael Goldblatt. Aerobiology and its role in the transmission of infectious diseases. *Journal of Pathogens*, 2013, 2013.